Substrate Recognition and Catalysis by UCH-L1†

Sarah J. Luchansky,*,‡ Peter T. Lansbury, Jr.,‡ and Ross L. Stein§

Center for Neurologic Diseases, Harvard Medical School and Brigham and Women's Hospital and Laboratory for Drug Discovery in Neurodegeneration, Harvard Center for Neurodegeneration and Repair, 65 Landsdowne Street, Fourth Floor, Cambridge, Massachusetts 02139

Received July 12, 2006; Revised Manuscript Received September 24, 2006

ABSTRACT: Deubiquitinating enzymes regulate essential cellular processes, and their dysregulation is implicated in multiple disease states. Ubiquitin carboxy-terminal hydrolase L1 (UCH-L1) has garnered attention for its links with Parkinson's disease and cancer; however, the mechanism of action of this enzyme in cells remains poorly understood. In order to advance our understanding of UCH-L1 function, we have been developing small molecule modulators of the enzyme for use as tools to probe its role in cells. In support of these efforts, an investigation of the mechanism of UCH-L1 catalysis was previously reported. Here, we extend this mechanistic evaluation and examine substrate recognition by UCH-L1. We developed a panel of ubiquitin fusions to test the contribution of specific residues of ubiquitin to binding and catalysis by the enzyme, and determined the activation parameters of selected variants to gain additional mechanistic insight. Ubiquitin side chains critical for establishing the Michaelis complex and enabling catalysis were identified, and features of this complex that differ between UCH-L1 and a homologue, UCH-L3, were revealed. These data provide dramatic examples of differences in substrate specificity between these enzymes. The implications of our experiments with UCH-L1 for selective inhibitor design and the relationship to disease are discussed.

Ubiquitination is essential to ensure the proper execution of cellular processes such as cell division, cell signaling and programmed cell death (*1*−*3*). Proteins destined for degradation or regulated by this post-translational modification are tagged with the ubiquitin protein (Ub[1]) through a series of enzymatic steps initiated by a Ub activating enzyme (E1). Following activation, Ub is delivered to a Ub conjugating enzyme (E2) and finally to a target protein in a process facilitated by an E3 ligase. Like other post-translational modifications (i.e., phosphorylation or glycosylation), Ub can also be readily removed from a target by a class of enzymes termed deubiquitinating enzymes (DUBs).

DUBs perform a number of distinct enzymatic reactions in the cell (*4*, *5*). These enzymes cleave polyubiquitin from target proteins, rescuing them from degradation, and hydrolyze monoubiquitin to influence downstream signaling pathways. DUBs also recycle free Ub, either from polyubiquitin chains or from small peptide conjugates. This protein family comprises ∼90 members that fall into the USP, UCH, MJD, OTU, and JAMM subclasses (*4*), of which the USP and UCH enzymes are the most well-characterized. Although progress is being made toward the identification of substrates for enzymes in the USP class, the identity of substrates and the cellular role of the UCH enzymes remain elusive. Tools enabling the functional investigation of this enzyme class such as cell-permeable small molecule inhibitors are highly coveted.

The most prominent UCH family member is UCH-L1, which has been genetically linked to Parkinson's disease (PD) (*6*, *7*) and is a component of the insoluble protein deposits (Lewy bodies) that occur in the brains of PD patients (*8*). UCH-L1 is also overexpressed in some cancerous tissues, including primary lung (*9*), colorectal (*10*), and pancreatic (*11*) cancers. To further our understanding of the role of UCH-L1 in both normal and diseased states, we are currently developing small molecule modulators to probe UCH-L1 function in cells (unpublished data and ref 12). In support of these efforts, we have been investigating the catalytic mechanism of UCH-L1 and have characterized some critical features of the cleavage of a Ub substrate, UbAMC, by the enzyme (*13*). In this article, we disclose additional features of UCH-L1 catalysis discovered by probing the molecular details of enzyme recognition with novel Ub substrates.

Herein, we describe UCH-L1 cleavage of a panel of Ub fusions designed to test the importance of specific residues of Ub to binding and catalysis by the enzyme. To gain further mechanistic insight into UCH-L1 catalysis, the activation parameters for hydrolysis of select Ub fusions by UCH-L1

† This research is supported by a grant from the Morris K. Udall Parkinson's Disease Research Center for Excellence. S.J.L. is supported by a Molecular Biology of Neurodegeneration Training Grant that is sponsored by the NIH and administered through the Harvard Center for Neurodegeneration and Repair.

* Corresponding author. Phone: (617) 768-8602. Fax: (617) 768-8606. E-mail: sarah.luchansky@gmail.com.

‡ Center for Neurologic Diseases, Harvard Medical School and Brigham and Women's Hospital.

§ Laboratory for Drug Discovery in Neurodegeneration.

[1] Abbreviations: AMC, 7-amido-4-methylcoumarin; AW, alanine-tryptophan peptide; DUB, deubiquitinating enzyme; Ub, ubiquitin; UbW, ubiquitin fused at the C-terminus to tryptophan; UbAW, ubiquitin fused at the C-terminus to alanine-tryptophan; UbWA, ubiquitin fused at the C-terminus to tryptophan-alanine; UCH, ubiquitin carboxy-terminal hydrolase; USP, ubiquitin specific protease; W, tryptophan; WA, tryptophan-alanine peptide.

10.1021/bi061406c CCC: $33.50
Published on Web 11/14/2006

were determined. Ub side chains critical for establishing the Michaelis complex and enabling catalysis were identified, and features of this complex that differ between UCH-L1 and its homologue, UCH-L3, were revealed. Although it is known that these related enzymes cleave Ub conjugates at dramatically different rates (*13*, *14*), we describe some variations in their substrate specificity that have not been previously observed.

MATERIALS AND METHODS

General. UCH-L1 and ubiquitin-AMC (UbAMC) were purchased from Boston Biochem. Buffer salts, tryptophan (W), alanine-tryptophan (AW), and tryptophan-alanine (WA) standards for reverse-phase HPLC were purchased from Sigma. Reverse-phase HPLC was performed on a Waters HPLC using a C8 reverse-phase column (Vydac, 2.1 × 100 mm). Tryptophan fluorescence was monitored with a Waters 474 fluorescence detector with excitation at 295 nm and emission at 353 nm. Reaction conditions for UbAMC hydrolysis by UCH enzymes were based on previously described procedures (*12*). The plasmid pGEX-6P-1, columns for glutathione affinity (GSTPrep FF 16/10 column) and ion exchange (HiTrap Q XL) chromatography as well as Prescission protease were purchased from Amersham Biosciences. CD spectroscopy was performed on an Aviv 62A DS spectropolarimeter. The CD spectra for each protein variant were measured in 1 nm intervals between 190 and 320 nm, and the values from three scans were averaged.

Cloning, Expression and Purification of UbW, UbAW, UbWA, and Variants. The genes coding for UbW, UbAW, and UbWA were generated by PCR from wild-type human Ub and cloned into pGEX-6P-1 using standard procedures. PCR mutagenesis to generate UbW variants was achieved with the QuikChange Site-Directed Mutagenesis Kit (Stratagene). The plasmids were transformed into BL21(DE3) *E. coli* cells, one colony was used to inoculate LB media containing 100 μg/mL ampicillin (10 mL), and the liquid culture was then used to inoculate 2−3 L of LB media containing 100 μg/mL ampicillin at 37 °C. Cells were grown to an $OD_{\lambda=600nm}$ of 0.4, 1 mM IPTG was added to induce protein expression, and the cultures were then incubated with shaking at 18 °C for 20 h. Following incubation, cells were harvested and lysed in PBS (pH 7.4) with a microfluidizer, and the lysate was subjected to centrifugation at 21000*g* for 1 h at 4 °C. The supernatants containing the GST fusion proteins were bound to a glutathione affinity chromatography column, the bound species were washed with PBS, and the protein was eluted with elution buffer (50 mM Tris•HCl, 150 mM NaCl, 1 mM EDTA, 10 mM reduced glutathione at pH 8.0). The elution fraction was concentrated to ∼10 mL and dialyzed overnight at 4 °C into PBS containing 1 mM DTT. During dialysis, the GST tag was cleaved from the fusion protein using Prescission protease (35 μL per 10 mL of elution buffer), cleaving all but five amino acids (GPLGS) from the N-terminus of Ub. Subsequently, the cleaved protein was separated from the GST tag using glutathione affinity chromatography as described above. The flow-through was dialyzed into 50 mM Tris•HCl and 0.5 mM EDTA at pH 7.6 and further purified using anion exchange chromatography with a linear gradient from 0 to 1 M NaCl. The purified protein was concentrated, dialyzed into PBS and stored at −80 °C. Prior to performing enzymatic assays, the absorbance of the solution at 280 nm was measured, and the concentration was calculated using a predicted extinction coefficient of 6970 M^{-1} cm^{-1}. The yield was typically 10 mg/L.

Determinations of the K_M Values of Ub Conjugate Variants with UCH-L1 and UCH-L3. The inhibition constants (K_I) for each Ub conjugate variant in the reaction between UbAMC and UCH-L1 or UCH-L3 were measured. UbAMC (30 nM with UCH-L1; 20 nM with UCH-L3) and multiple concentrations of UbW, UbAW, UbWA, or the UbW variants were mixed in reaction buffer (50 mM Tris•HCl, 0.5 mM EDTA, 5 mM DTT, and 0.5 mg/mL ovalbumin) and UCH-L1 (1 nM final concentration) or UCH-L3 (activated by preincubation with reaction buffer for 5 min; 2 pM final concentration) was added to initiate the enzymatic reaction (100 μL final volume). The rate of AMC cleavage was monitored at 25 °C with a Molecular Devices Gemini XS microplate spectrofluorometer with excitation at 355 nm and emission at 450 nm. Initial reaction rates were calculated by Softmax and then plotted versus the Ub variant concentration using the program GraphPad Prism. Values for $K_{I,app}$ were obtained by curve fitting to the average of three replicates, and the K_I values were determined from the $K_{I,app}$ parameters as described in the Results section. The K_M values for each conjugate are equal to the K_I values. For each variant, the K_M value reported is the average from at least three independent measurements, and the standard deviations were between 4 and 20% of the mean.

Determinations of the k_c Values of Ub Conjugate Variants with UCH-L1 and UCH-L3 Using HPLC. UbW, UbAW, UbWA, or UbW variants (typically at concentrations at least 20 times the K_M value) were incubated with UCH-L1 (10 nM−1 μM) or UCH-L3 (100 pM−2 nM) in reaction buffer (1 mL final volume, 50 mM Tris•HCl, 0.5 mM EDTA, and 5 mM DTT) for 1 h at 25 °C. At 5 min intervals, aliquots were removed (50 μL) and quenched with 500 mM acetic acid (10 μL) (*12*). W (or AW or WA) was separated from the reaction mixture by reverse-phase HPLC using a gradient of acetonitrile (10−70%) and water and monitored with fluorescence detection. The concentration of W (or AW or WA) was determined by integration of each peak and comparison with a standard curve. For UbW variants with a high K_M, k_c and k_c/K_M values were determined from the standard Michaelis−Menten equation under conditions in which the [UbW] was in slight excess of K_M or much less than K_M, respectively. Each value of k_c was determined three times, and the average of these values was reported. The standard deviations of k_c were between 3 and 20% of the mean.

Temperature Dependencies of k_c for UbW, UbAW, and $Ub^{G76A}W$ with UCH-L1. UbW (10 μM), UbAW (10 μM), or $Ub^{G76A}W$ (39 μM) was incubated with UCH-L1 (10 nM, 2 μM, or 400 nM, respectively) in reaction buffer (50 mM HEPES, 0.5 mM EDTA, and 5 mM DTT) at a temperature ranging from 10 − 40 °C. Decreased UCH-L1 activity was observed at higher temperatures (*13*). The reaction time was varied to capture the initial rate of each reaction. At the appropriate intervals, 50 μL of the reaction mixture was removed, quenched with 10 μL of 500 mM acetic acid and analyzed by HPLC as described in the previous section. The k_c values at each temperature were determined at least three times, and the data were combined to generate an Eyring

plot for each variant. The activation parameters were determined from these plots as described in the Discussion section.

RESULTS

Identification of a Ub Conjugate Scaffold for Mutagenesis. To measure the importance of specific residues of Ub to binding and catalysis by UCH-L1, we sought a scaffold on which to install point mutations in the Ub moiety. Although UbAMC is a common substrate for the UCH enzymes, the derivatization of Ub with Gly-Gly-AMC in the presence of trypsin (*15*) is typically a low-yielding and labor-intensive synthesis. To simplify the generation of multiple Ub conjugate variants, we introduced a natural amino acid fluorophore (tryptophan) at the C-terminus of Ub. Derivatization steps following the expression and purification of the protein could be avoided with this approach.

Because the preference of UCH-L1 for a tryptophan at the C-terminus of Ub was unknown, we expressed Ub as a C-terminal fusion with either tryptophan (UbW) or alanine-tryptophan (UbAW). Both proteins were expressed in *E. coli* with removable N-terminal GST tags to facilitate purification. After a series of affinity and ion exchange chromatography purification steps, UbW and UbAW were obtained in high purity and good yield (Figure 1A).

The K_M values for UbW and UbAW with UCH-L1 were determined by treating these fusions as inhibitors of the reaction between UbAMC and UCH-L1. By measuring the dependence of the rate of AMC release on UbW (or UbAW) concentration (Figure 1B), the apparent inhibition constants ($K_{I,app}$) were determined from the concentration of UbW for which the rate of AMC release is half-maximum. Because Ub itself is a competitive inhibitor of this reaction (*13*), we assume that UbW and UbAW are also likely to exhibit this pattern of inhibition. Therefore, the inhibition constants (K_I) for UbW (and UbAW) can be determined from the following equation relating the K_I and $K_{I,app}$ values for a competitive inhibitor

$$K_I = \frac{K_{I,app}}{1 + \frac{[S_o']}{K_M'}} \quad \text{and} \quad K_M = K_I \qquad (1)$$

in which $K_M' = K_M$ for UbAMC and $[S_o'] = [UbAMC_o]$. The K_M values when UbW and UbAW are substrates are equal to the K_I values obtained from eq 1 and are presented in comparison with the parameters for the known substrate, UbAMC (Table 1).

Unlike UbAMC, which is nonfluorescent until release of the coumarin moiety by enzymatic cleavage, UbW and UbAW are similar in fluorescence intensity to tryptophan (W) and alanine-tryptophan (AW), respectively (data not shown). Therefore, to analyze UCH-L1 cleavage of these substrates, we developed an HPLC assay to observe the appearance of W and AW, respectively. A progress curve for the reaction of UCH-L1 with either UbW or UbAW was generated by removing aliquots from each mixture, quenching them, and separating each component by reverse-phase HPLC with fluorescence detection (Figure 1C). The catalytic rate constants (k_c) for UbW and UbAW with UCH-L1 were determined under reaction conditions in which $[S] \gg K_M$, where $[S] = [UbW]$ or $[UbAW]$ and K_M is the Michaelis constant for each conjugate (described above). Under these conditions, $v_0 = k_c[E_0]$, where v_0 = initial rate and $[E_0] =$

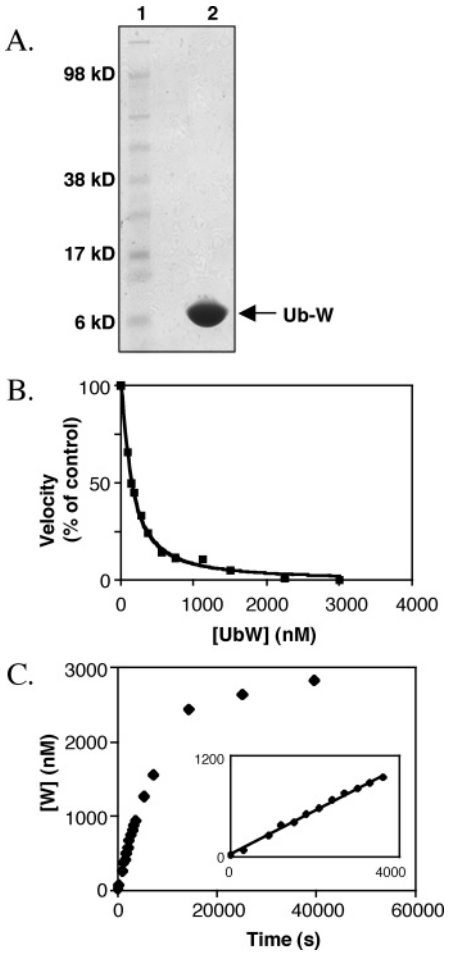

FIGURE 1: Expression of UbW and its reaction with UCH-L1. (A) SDS−PAGE gel showing purified UbW. The conjugate was expressed as a GST fusion protein, and the tag was removed prior to the final purification steps. Lane 1, molecular weight marker; lane 2, purified UbW. (B) Plot showing the velocity of UbAMC cleavage by UCH-L1 vs [UbW]. The velocity is expressed as a percent compared with that of the reaction where [UbW] = 0. Each data point represents the average of three measurements. The curve fit was generated by nonlinear regression analysis using the program Graphpad Prism from which a $K_{I,app}$ value for UbW was determined. The $K_{I,app}$ value was converted into a K_I value using eq 1 as described in the text. (C) Reaction progress curve showing [W] vs time for the cleavage of UbW by UCH-L1. The inset shows early time points from which an initial velocity was calculated. The catalytic rate constant (k_c) was determined from the initial velocity as described in the text. The data shown for UbW in A−C are representative of experiments with the other Ub conjugate variants.

Table 1: Kinetic Parameters of Ub Fusions with UCH-L1[a]

Ub variant	$K_M = K_S$[b] (μ**M**)	$k_c = k_2$ (s^{-1})	$k_c/K_M = k_2/K_S$ ($\times$ **10**^{4} M^{-1} s^{-1})
UbW	0.13	0.03[c]	19.7
UbAW	0.08	0.0001[c]	0.1
UbWA	0.45	0.0005[c]	0.1
UbAMC	0.04	0.02[b]	51.0

[a] See the Discussion section for an interpretation of the kinetic parameters. [b] Reaction conditions: 50 mM Tris•HCl, 0.5 mM EDTA, 0.5 mg/mL ovalbumin, 5 mM DTT at pH 7.6 at 25 °C. [c] Reaction conditions: 50 mM Tris•HCl, 0.5 mM EDTA, 5 mM DTT at pH 7.6 at 25 °C.

Table 2: Kinetic Parameters of Ub Fusions with UCH-L3[a]

Ub variant	K_M[b] (μM)	k_c (s^{-1})	$k_c/K_M = k_2/K_S$ ($\times 10^4$ M^{-1} s^{-1})
UbW	0.20	2.6[c]	1301
UbAW	0.16	1.5[c]	949
UbWA	0.78	2.4[c]	304
UbAMC	0.02	5.9[b]	27730

[a] See the Discussion section for an interpretation of the kinetic parameters. [b] Reaction conditions: 50 mM Tris•HCl, 0.5 mM EDTA, 0.5 mg/mL ovalbumin, 5 mM DTT at pH 7.6 at 25 °C. [c] Reaction conditions: 50 mM Tris•HCl, 0.5 mM EDTA, 5 mM DTT at pH 7.6 at 25 °C.

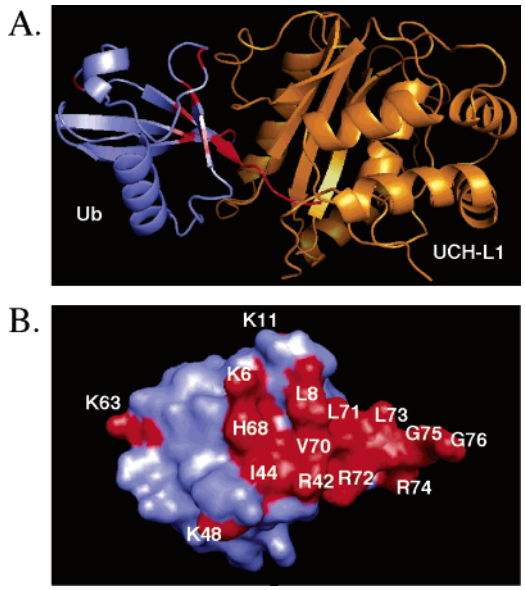

FIGURE 2: Ub mutants generated to probe the Ub/UCH-L1 interface. (A) Model of UCH-L1 (orange) with UbVME (blue) generated from the co-crystal structure of UCH-L3 with UbVME (*17*). Residues of Ub that were mutated to alanine are shown in red. (B) Surface map of the structure of Ub (blue) rotated to reveal the interface that contacts UCH-L1. The residues indicated in red were mutated to alanine. The Figure was generated using MacPyMOL.

initial enzyme concentration. From the early time points of the reaction, v_0 was calculated for each substrate, and k_c parameters were determined (Table 1). We also generated a Ub conjugate in which the peptide tryptophan-alanine was fused to the C-terminus of Ub (UbWA), and the kinetic parameters (K_M and k_c) with UCH-L1 (Table 1) were determined as described above. For comparison, UCH-L3 hydrolyses of UbW, UbAW, and UbWA were also examined (Table 2). On the basis of the fact that UbW is a competent substrate for both enzymes, whereas UbAW and UbWA are poor substrates for UCH-L1, we selected UbW as a scaffold for subsequent mutagenesis.

Mutagenesis of the Ub Moiety of UbW. Previous mutagenesis and crystallographic experiments have provided a picture of the interaction between Ub and either UCH-L3 or a yeast homologue (Yuh1) (*16*−*19*) and suggest that UCH-L1 (*20*) interacts with its substrates in a similar fashion. These data as well as functional analyses related to other interacting partners (*21*) have focused our mutagenesis of UbW to specific regions of the protein. The mutated residues are mainly located in two distinct regions of Ub (Figure 2 and Tables 3 and 4), which, together, make up the interface that contacts UCH-L3, Yuh1, and, most likely, UCH-L1. To

Table 3: Kinetic Parameters of UbW Variants with UCH-L1[a]

UbW variants	$K_M = K_S$[b] (μM)	$k_c = k_2$[c] (s^{-1})	$k_c/K_M = k_2/K_S$ ($\times 10^4$ M^{-1} s^{-1})	$(k_2/K_S)_{variant}/(k_2/K_S)_{wt}$
wild type	0.1	0.03	19.7	N.A.
K6A	0.9	0.03	3.9	0.20
L8A	>30	N.D.	0.1[c]	0.003
K11A	1.1	0.03	2.7	0.14
R42A	0.1	0.02	30.8	1.57
I44A	3.1	0.09	2.8	0.14
K48A	0.3	0.04	11.9	0.60
K63A	0.4	0.03	6.7	0.34
H68A	0.5	0.06	10.0	0.52
V70A	0.6	0.05	7.8	0.40
L71A	8.0	0.03	0.3	0.02
R72A	0.6	0.03	5.4	0.27
L73A	5.8	0.01	0.2	0.01
R74A	0.2	0.01	6.3	0.32
G75A	0.1	0.01	21.7	1.10
G76A	2.0	0.0011	0.1	0.003

[a] See the Discussion section for an interpretation of the kinetic parameters. [b] Reaction conditions: 50 mM Tris•HCl, 0.5 mM EDTA, 0.5 mg/mL ovalbumin, 5 mM DTT at pH 7.6 at 25 °C. [c] Reaction conditions: 50 mM Tris•HCl, 0.5 mM EDTA, 5 mM DTT at pH 7.6 at 25 °C.

Table 4: Kinetic Parameters of UbW Variants with UCH-L3[a]

UbW variants	K_M[b] (μM)	k_c[c] (s^{-1})	$k_c/K_M = k_2/K_S$ ($\times 10^4$ M^{-1} s^{-1})	$(k_2/K_S)_{variant}/(k_2/K_S)_{wt}$
wild type	0.2	2.6	1302.0	N.A.
K6A	1.4	4.0	275.0	0.21
L8A	28.2	6.6	23.6	0.02
K11A	2.3	3.4	149.1	0.12
R42A	0.1	0.2	499.1	0.38
I44A	0.4	1.6	383.0	0.29
K48A	0.7	2.4	333.1	0.26
K63A	0.8	2.4	323.0	0.25
H68A	0.5	4.6	960.0	0.74
V70A	1.1	6.7	636.0	0.49
L71A	19.8	9.2	46.2	0.04
R72A	1.9	4.4	227.0	0.18
L73A	10.4	5.7	54.7	0.04
R74A	4.5	0.3	6.5	0.01
G75A	0.4	2.9	727.0	0.56
G76A	1.1	1.7	159.4	0.12

[a] See the Discussion section for an interpretation of the kinetic parameters. [b] Reaction conditions: 50 mM Tris•HCl, 0.5 mM EDTA, 0.5 mg/mL ovalbumin, 5 mM DTT at pH 7.6 at 25 °C. [c] Reaction conditions: 50 mM Tris•HCl, 0.5 mM EDTA, 5 mM DTT, pH 7.6 at 25 °C.

determine the importance of specific side chains of Ub during the cleavage reaction catalyzed by UCH-L1, we performed a directed alanine scan and generated 15 point mutants of UbW using site-directed mutagenesis. We included K48 and K63 to determine whether these commonly elaborated lysines on Ub are critical for interaction with UCH-L1.

UCH Cleavage of UbW Variants. UbW variants were expressed and purified as described earlier for the wild-type protein. Like UbW, all mutants were present in the soluble fraction upon lysis of the *E. coli* cells and were structurally identical to UbW when analyzed by CD spectroscopy (data not shown). Next, the K_M and k_c values for the UbW variants with both UCH-L1 and UCH-L3 were determined as described above for the wild-type protein (Tables 3 and 4).

Temperature Dependencies of UCH-L1 Cleavage of UbW, UbAW, and Ub^{G76A}W. UbAW and Ub^{G76A}W had significantly lower catalytic rate constants (k_c) than UbW with UCH-L1,

indicating that the enzyme hydrolyzed these variants slowly (Tables 1 and 3). We further investigated the decreased rate of catalysis by monitoring k_c at various temperatures. According to transition state theory, the first-order rate constant, k_c, will have the following dependence on temperature.

$$k_c = \kappa \frac{k_B T}{h} \exp\left(-\frac{\Delta G^{\ddagger}}{RT}\right) \quad (2)$$

In eq 2, $\Delta G^{\ddagger}$, κ, k_B, h, and R are the Gibbs free energy of activation, the transmission coefficient, and the Boltzmann, Planck, and gas constants, respectively. This equation can be rewritten as follows:

$$k_c = \kappa \frac{k_B T}{h} \exp\left(-\frac{\Delta H^{\ddagger}}{RT} + \frac{\Delta S^{\ddagger}}{R}\right) \quad (3)$$

$\Delta H^{\ddagger}$ and $\Delta S^{\ddagger}$ are equal to the enthalpy and entropy of activation, respectively. In eq 3, the transmission coefficient is assumed to be equal to 1. We can then rearrange eq 3 to eq 4,

$$\ln\left[k_c\left(\frac{h}{k_B T}\right)\right] = -\frac{\Delta H^{\ddagger}}{RT} + \frac{\Delta S^{\ddagger}}{R} \quad (4)$$

which predicts that a plot of $\ln[k_c(h/(k_B T))]$ versus inverse temperature (Eyring plot) will be linear with a slope and an intercept proportional to $\Delta H^{\ddagger}$ and $\Delta S^{\ddagger}$, respectively. The temperature dependencies of k_c for UbW, UbAW, and Ub^{G76A}W were analyzed in this manner (Figure 3), and the activation parameters are reported in Table 5.

DISCUSSION

General Comments on the Mechanism of UCH-L1 and the Interpretation of Mutagenesis Data. UbAMC cleavage by UCH-L1 and UCH-L3 is believed to proceed through the pathway outlined in Scheme 1, and the reaction rate is governed by the Michaelis equation such that the steady-state rate constants are equal to the following, as represented in eqs 5−7.

$$k_c = \frac{k_2 k_3}{k_2 + k_3} \quad (5)$$

$$K_M = K_S\left(\frac{k_3}{k_2 + k_3}\right) \quad (6)$$

$$\frac{k_c}{K_M} = \frac{k_2}{K_S} \quad (7)$$

Here, $K_S = (k_{-1} + k_2)/k_1$, which simplifies to $K_S = k_{-1}/k_1$ for most amide bond hydrolysis reactions. We previously reported a mechanistic evaluation of the catalytic reaction between UCH-L1 and UbAMC (*13*). For this reaction, our results indicated that $k_c = k_2$; in other words, the formation of the acyl-enzyme intermediate is the rate-limiting step to catalysis (*13*). In this situation, when $k_2 \ll k_3$, then $K_S = K_M$. Because the kinetic parameters for the cleavage of UbW by UCH-L1 closely resemble those of UbAMC, it is likely that the cleavage of both ubiquitinated species proceed through a similar mechanism. Therefore, decreases in k_c for UbW variants hydrolyzed by UCH-L1 reflect changes during the acylation step. In support of this assumption, we were able to rule out deacylation as the rate-limiting step for slowly hydrolyzed UbW variants (see below). Furthermore, because

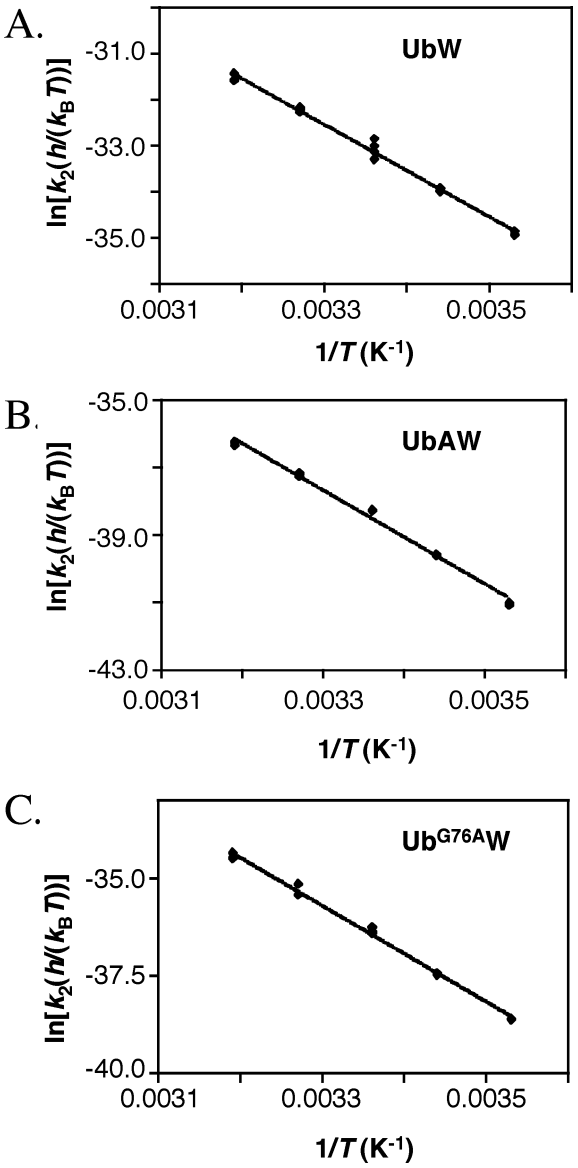

FIGURE 3: Temperature dependencies for Ub conjugate variants with UCH-L1. The Eyring plots show the dependence of k_2 on temperature for UCH-L1 cleavage of UbW (A), UbAW (B), and Ub^{G76A}W (C). For each variant, k_2 was determined at least three times at each temperature. The data were fit to a line using the program GraphPad Prism. Activation parameters were determined from the slopes, and *y*-intercepts of the lines and are reported in Table 5. The symbols h and k_B represent the Planck and Boltzmann constants, respectively.

Table 5: Activation Energy Parameters of k_c[a] for Ub Conjugate Variants with UCH-L1

Ub variant[b]	$\Delta G^{\ddagger}$	$\Delta H^{\ddagger}$	$\Delta S^{\ddagger}$	$-T\Delta S^{\ddagger}$[f]
UbW[c]	19.6 ± 0.7	19.9 ± 0.5	0.001 ± 0.001	−0.3 ± 0.5
Ub^{G76A}W[d]	21.3 ± 0.6	24.4 ± 0.4	0.010 ± 0.001	−2.9 ± 0.5
UbAW[e]	22.7 ± 1.1	27.6 ± 0.9	0.016 ± 0.002	−4.9 ± 0.7

[a] $k_c = k_2$. [b] Reaction conditions: 50 mM HEPES, 0.5 mM EDTA, 5 mM DTT at pH 7.6. Units for $\Delta G^{\ddagger}$, $\Delta H^{\ddagger}$, and $-T\Delta S^{\ddagger}$ are kcal/mol; units for $\Delta S^{\ddagger}$ are cal/mol/K. [c] [UbW] = 10 μM; [UCH-L1] = 10 nM. [d] [Ub^{G76A}W] = 39 μM; [UCH-L1] = 400 nM. [e] [UbAW] = 10 μM; [UCH-L1] = 2 μM. [f] T = 303 K.

Scheme 1: Minimal Kinetic Mechanism for UCH Enzymes[a]

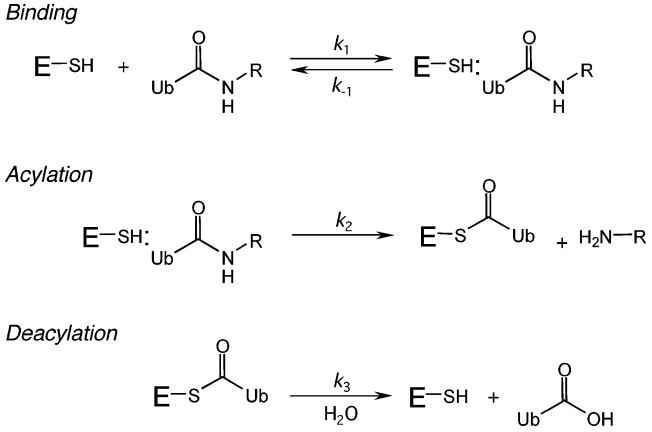

[a] R = small molecule or peptide.

the K_M value for each Ub conjugate with UCH-L1 is equal to the dissociation constant of the Michaelis complex (K_S), perturbations to K_M (but not k_c) for a UbW variant indicate that this residue is important mainly for complex formation.

In contrast to UCH-L1, UCH-L3 hydrolysis of UbAMC may be limited by the rate of deacylation ($k_c = k_3$) (*15*). Further efforts are needed to clarify the relative magnitudes of k_2 and k_3 for this reaction; therefore, we will not attempt to interpret the meaning of k_c for UCH-L3 in terms of individual steps. Rather, the overall second-order rate constants (k_2/K_S) can be used to compare the cleavage efficiencies of UCH-L1 and UCH-L3.

Identification of a Ub Conjugate Scaffold for Mutagenesis. To facilitate the generation of a number of Ub conjugate variants, we designed a Ub substrate containing a cleavable tryptophan fluorophore at the C-terminus. Because both the substrate and product are fluorescent, an HPLC assay was developed to monitor these reactions. Although this method of detection provides lower throughput than a fluorogenic assay, we felt this approach was advantageous because the generation of AMC-derivatized Ub can be laborious. Furthermore, Ub conjugate variants, rather than mutants of Ub alone, were required to evaluate which residues make important interactions during both catalysis and enzyme−substrate complex formation.

K_M values for enzymatic reactions are typically measured by determining the reaction velocity at multiple substrate concentrations. With an HPLC assay, this approach is particularly labor-intensive. We simplified the K_M determinations by measuring the K_I values for UbW, its variants, UbAW, and UbWA in the reaction between UbAMC and UCH-L1 (see above, Figure 1 and Tables 1−4). By definition, the K_I values for these variants as inhibitors are equal to the K_M values when they are substrates. The K_M value for UbW with UCH-L1 (0.1 μM) was identical to the K_I value for Ub itself (data not shown), suggesting that the C-terminal tryptophan of UbW does not significantly affect binding to the enzyme. Cleavage of the Ub conjugate variants by both UCH-L1 and UCH-L3 was measured using the HPLC assay, and the k_c values were extracted from these analyses (Tables 1−4). Although the experiments were typically run under conditions in which [S] $\gg K_M$ (Results section), the K_M value for $Ub^{L8A}W$ with UCH-L1 was too high to be measured (K_M > 30 μM). In this case, the reaction was performed under conditions in which [S] $\ll K_M$ such that $k_c/K_M = v_0/[E_0]$. Neither k_c nor K_M was individually determined. In other cases where K_M was high ($Ub^{L71A}W$, $Ub^{L73A}W$ and $Ub^{R74A}W$), the enzymatic reactions were run under conditions in which [S] > K_M such that

$$k_c = \frac{v_0}{[E_0]}\left(\frac{K_M + [S]}{[S]}\right) \quad (8)$$

Although the substrate preferences of UCH-L1 and UCH-L3 for some Ub conjugates have been examined (*14*), the preference of either of these enzymes for tryptophan at the C-terminus of Ub was unknown. Therefore, we tested both UbW and UbAW as substrates for UCH-L1, considering that a bulky residue following Ub might be unfavorable. To our surprise, UbW was hydrolyzed much more rapidly by UCH-L1 than UbAW. There was a 200-fold difference in the k_2/K_S parameter between the variants, and this difference is entirely due to a change in k_c (Table 1). In contrast, UCH-L3 cleaved UbW and UbAW at similar rates (Table 2). Although the overall cleavage efficiency of UCH-L3 with Ub conjugates *in vitro* is consistently greater than that of UCH-L1, the enzymes typically show similar patterns of substrate recognition (*13*−*15*, *22*). Our data provide novel examples of Ub substrates for which UCH-L1 and UCH-L3 show a significantly different cleavage pattern.

We undertook two experiments to probe the mechanistic basis of the preference of UCH-L1 for UbW over UbAW. To identify the enthalpic and entropic contributions during the cleavage step, we measured the temperature dependencies of these reactions, as discussed below. Second, we wished to distinguish between two modes of UCH-L1 recognition suggested by these substrates. It has previously been reported that UCH-L1 poorly cleaves ubiquitin fused to short peptides (8−10 amino acids), whereas UCH-L3 accomplishes this cleavage more efficiently (*14*). The poor cleavage of UbAW by UCH-L1 may indicate that the enzyme does not efficiently recognize Ub conjugates with two amino acid C-terminal extensions or, alternatively, that UCH-L1 has a preference against large amino acids in the P2′ position. To distinguish between these possibilities, we generated the conjugate UbWA and measured its kinetic parameters with UCH-L1 and UCH-L3 (Tables 1 and 2). As expected, UCH-L3 hydrolyzed UbWA with high efficiency, consistent with previous observations (*14*) and the notion that this enzyme is fairly promiscuous, cleaving two amino acid C-terminal extensions of Ub with relatively little amino acid preference. The kinetic parameters for UCH-L1 with UbWA, however, resemble those with UbAW and suggest that this enzyme has a preference against two amino acid C-terminal extensions of Ub, regardless of the amino acid at the P2′ position. UCH-L1 has not been shown to cleave ubiquitinated proteins, with Ub linked either through an isopeptide bond to the ϵ-amine of a lysine residue or through a peptide bond as an α-amine-linked fusion protein. Our observations support the contention that UCH-L1 is unable to cleave α-linked Ub fusion proteins. Whether this enzyme, like UCH-L3 (*17*), can hydrolyze Ub conjugated to a C-terminal peptide through an isopeptide bond remains unknown and was not addressed in our experiments. The isopeptide linkage would present the surrounding amino acids in a drastically different

geometry from that of the peptide bond; therefore, these substrates may be sterically permitted.

Mutagenesis of the Ub Moiety of UbW. Mutagenesis of amino acids in the Ub moiety of UbW was undertaken to identify residues of the protein important for the formation of the enzyme−substrate complex with UCH-L1 (manifested in changes to K_S) as well as during the acylation step (manifested in changes to k_2). We chose to perform a directed alanine scan because this method typically enables the assessment of contributions of specific side chains without the introduction of unnatural backbone flexibility or destabilization due to steric or electrostatic factors (*21*, *23*, *24*). In this case, the mutation of G75 and G76 of Ub to alanine results in an increase in steric bulk and a decrease in backbone flexibility; however, we included these mutations to dissect the mechanism behind the specificity of the UCH enzymes for these two residues.

Many UbW variants with UCH-L1 exhibited only modest changes in K_S (<10-fold) compared with UbW. The largest increase in this parameter (>300-fold) resulted from the mutation of a leucine at position 8 to alanine ($Ub^{L8A}W$). Although we were unable to precisely determine this parameter, the large increase in K_S compared with that of wild-type UbW indicates that leucine 8 is critical for the formation of the Michaelis complex. Substitution of the leucine residues at positions 71 and 73 with alanine ($Ub^{L71A}W$ and $Ub^{L73A}W$) also significantly altered the K_S with UCH-L1. All three of these residues are thought to be involved in hydrophobic interactions with UCH-L3 (Table 4 and ref 16) and Yuh1 (*17*, *19*), and our data suggest that the same is true for UCH-L1.

The only other UbW variants with large increases in K_S with UCH-L1 (>10-fold) were $Ub^{I44A}W$ (30-fold) and $Ub^{G76A}W$ (20-fold). Residue 44 of UbW is important for Michaelis complex formation with UCH-L1 but less important in the transition state because k_2 is unaffected. Interestingly, $Ub^{I44A}W$ behaves like the wild-type conjugate with UCH-L3, suggesting that the interfaces of these two enzymes with their substrates are not identical. This feature is not obvious from the structural data available and suggests that selective inhibitors of UCH-L1 may be achievable. When the final residue of Ub is an alanine ($Ub^{G76A}W$), there are 20- and 5-fold increases in K_S with UCH-L1 and UCH-L3, respectively; however, the catalytic rate constant (k_c) is only affected for UCH-L1. The different effects on k_c with the two enzymes may arise from the fact that k_c does not reflect the same catalytic step for these enzymes (i.e., acylation for UCH-L1 and deacylation for UCH-L3), and glycine 76 may play a different role during these steps. Alternatively, if acylation is rate-limiting for UCH-L3, the change in k_c with UCH-L1, but not UCH-L3, may indicate a structural difference between these two enzymes during the transition state leading to the acyl-enzyme. Future clarification of the rate-limiting step of UbAMC and UbW hydrolysis by UCH-L3 will help to resolve this point. Interestingly, the rate of UCH-L1 cleavage of $Ub^{G75A}W$ resembled that of the wild-type protein, suggesting that only the final glycine residue of Ub is a critical determinant for UCH-L1 recognition.

We observed altered k_c values for the hydrolyses of two other Ub variants, $Ub^{R74A}W$ and $Ub^{R42A}W$, by UCH-L3 but not UCH-L1. Both of these proteins, compared with that of the wild-type UbW, showed significantly reduced catalytic rate constants with UCH-L3, and the K_M for $Ub^{R74A}W$ was also increased. R42 is located far from the cleavage site and may be involved in a conformational change required for catalysis by UCH-L3. In contrast, the arginine side chain of R74 makes multiple contacts to residues of UCH-L3 in the co-crystal structure (*17*). Consequently, the near-wild-type efficiency of UCH-L1 cleavage of $Ub^{R74A}W$ is surprising, although some of the residues important for contacting R74 vary between the two enzymes. Overall, the different selectivities of UCH-L1 and UCH-L3 for the residues at positions 42, 74, and 76 of UbW suggest that the C-terminus of Ub interacts differently with each enzyme during catalysis.

We next considered the dependence of UCH-L1 cleavage of Ub fusions on temperature. For the reaction of UbAMC with UCH-L1, the activation parameters determined from the temperature dependence of the acylation step revealed an enthalpy of activation equal to 20 kcal/mol and an entropy of activation essentially equal to zero (*13*). We proposed that this minimal entropy change indicates a pre-organization mechanism, in which UCH-L1 and UbAMC in the Michaelis complex are optimally oriented for catalysis (*13*). To determine whether this is a general mechanism of UCH-L1 catalysis, we investigated the temperature dependence of k_2 for the UCH-L1-catalyzed cleavage of UbW and generated an Eyring plot to determine the activation parameters (Figure 3A). The plot is linear, indicating that no observable change in mechanism occurs with temperature, and the acylation of both UbW and UbAMC by UCH-L1 proceeds with similar changes in the enthalpy and entropy (Table 5 and ref 13). This observation is consistent with the idea that rate-limiting acylation is characterized by pre-organization of the Michaelis complex for UbW and suggests that this is a general mechanism employed by UCH-L1.

Two Ub conjugate variants that showed a significant alteration to k_c with UCH-L1/UbAW and $Ub^{G76A}W$ were identified. The decrease in k_c is not due to a change in the rate-limiting step of catalysis from acylation to deacylation. Under the conditions of our experiments, we would have been able to observe a pre-steady-state burst, indicating a slow deacylation step; however, that was not observed for either substrate (data not shown). Therefore, k_c is equal to k_2 for UbAW and $Ub^{G76A}W$. To further our understanding of the mechanism behind the changes to the catalytic rate constants for these variants, we measured k_2 at multiple temperatures for UbAW and $Ub^{G76A}W$ and generated Eyring plots (Figure 3B and C). We noted that the acylation of UCH-L1 by UbW, UbAW, and $Ub^{G76A}W$ occurs with distinctly different activation parameters (Table 5). That is, while acylation by UbW proceeds with an enthalpy of activation ($\Delta H^{\ddagger}$) of 19.9 kcal/mol and no entropy of activation ($\Delta S^{\ddagger}$), UbAW and $Ub^{G76A}W$ both acylate UCH-L1 with larger changes in the enthalpy ($\Delta H^{\ddagger}$ > 24 kcal/mol) that are partially offset by large, favorable entropy changes ($\Delta S^{\ddagger}$ > 0). It is not immediately obvious how to explain the differences between the reactions of these Ub conjugate variants, given that in each case, acylation ostensibly proceeds by precisely the same mechanism and through the same transition state. Clearly, if such differences cannot be attributed to the substrate-derived portion of the transition state, then they must have their origins in the protein-derived portion.

We propose that as the Michaelis complex for each Ub variant proceeds to the transition state for acylation, the chemistry of acylation occurs (i.e., attack of the UCH-L1 active-site cysteine on the carbonyl carbon of the Ub substrate) along with adjustments in the composition of the ensemble of conformational isomers or substates that comprise the complex. As the transition state is entered, one can imagine that the composition of this ensemble will change and reflect only those substates that can support acylation chemistry. Changes to the structure of the Ub conjugate (i.e., UbAW and $Ub^{G76A}W$) will likely change the composition of the Michaelis complex ensemble. Furthermore, if structural features of certain variants preclude the formation of catalytically optimal transition state substates, catalytic efficiency will be diminished for this Ub conjugate. This is, of course, the protein-structural basis for substrate selectivity.

The differences in activation parameters that we see for the acylation of UCH-L1 by UbW, $Ub^{G76A}W$, and UbAW can, thus, be attributed to differences in the composition of the ensemble of protein conformations that proceeds from the Michaelis complex to the acyl-enzyme for each variant. For example, during the acylation of UCH-L1 by UbW, it is apparently the case that the only conformations of the UCH-L1/UbW ensemble that will enter the transition state are those in which the thiolate of the active site cysteine residue and the substrate's carbonyl carbon are perfectly aligned. As mentioned above, in this transition state, no further adjustment of protein conformational state needs to occur, and catalysis proceeds through a pre-organization mechanism. In contrast, during the acylation of UCH-L1 by UbAW or $Ub^{G76A}W$, the relative concentration of conformational isomers in the ensemble that support optimal alignment of the thiolate and carbonyl carbon is low. Furthermore, those conformational isomers of the Michaelis complex that are catalytically competent are apparently more strained than the transition state they will ultimately enter. Combined, these factors lead to a larger enthalpy of activation and a more favorable entropy of activation for the acylation of UCH-L1 by $Ub^{G76A}W$ or UbAW, relative to the acylation by Ub-W. Overall, these observations emphasize the importance of a highly organized complex between UCH-L1 and its substrate in order to achieve reasonable catalytic efficiency.

In conclusion, we designed novel substrates for UCH-L1, UbW, UbAW, and UbWA and generated 15 point mutants of the UbW conjugate to probe the importance of specific residues of Ub to binding and catalysis by the enzyme. We identified L8, L71, and L73 of UbW as important determinants of Michaelis complex formation with either UCH-L1 or its homologue, UCH-L3. Interestingly, the two enzymes differed in their recognition of $Ub^{R42A}W$, $Ub^{I44A}W$, $Ub^{R74A}W$, $Ub^{G76A}W$, and two other fusions, UbAW and UbWA. Our observations indicate that UCH-L1 and UCH-L3 interact differently with Ub conjugates and imply that the generation of selective inhibitors for each enzyme should be achievable. Furthermore, there appear to be structural variations in the transition states of these enzymes during catalysis. For UCH-L1 in particular, further mechanistic evaluation of select Ub fusions reinforced the importance of a pre-organized Michaelis complex to UCH-L1 catalysis. Our data provide some dramatic examples of differences in patterns of substrate specificity between the UCH enzymes and suggest that overall differences in substrate preference may contribute to the link of UCH-L1, but not UCH-L3, with PD, and cancer.

ACKNOWLEDGMENT

We thank Yichin Liu and Hilal Lashuel for purified UCH-L3 and Chittaranjan Das for assistance with the structural analysis of UCH-L1.

REFERENCES

1. Hershko, A., and Ciechanover, A. (1998) The ubiquitin system, *Annu. Rev. Biochem. 67*, 425−479.
2. Pickart, C. M. (2001) Mechanisms underlying ubiquitination, *Annu. Rev. Biochem. 70*, 503−533.
3. Hicke, L. (2001) Protein regulation by monoubiquitin, *Nat. Rev. Mol. Cell Biol. 2*, 195−201.
4. Nijman, S. M., Luna-Vargas, M. P., Velds, A., Brummelkamp, T. R., Dirac, A. M., Sixma, T. K., and Bernards, R. (2005) A genomic and functional inventory of deubiquitinating enzymes, *Cell 123*, 773−786.
5. Amerik, A. Y., and Hochstrasser, M. (2004) Mechanism and function of deubiquitinating enzymes, *Biochim. Biophys. Acta. 1695*, 189−207.
6. Leroy, E., Boyer, R., Auburger, G., Leube, B., Ulm, G., Mezey, E., Harta, G., Brownstein, M. J., Jonnalagada, S., Chernova, T., Dehejia, A., Lavedan, C., Gasser, T., Steinbach, P. J., Wilkinson, K. D., and Polymeropoulos, M. H. (1998) The ubiquitin pathway in Parkinson's disease, *Nature 395*, 451−452.
7. Maraganore, D. M., Lesnick, T. G., Elbaz, A., Chartier-Harlin, M. C., Gasser, T., Kruger, R., Hattori, N., Mellick, G. D., Quattrone, A., Satoh, J., Toda, T., Wang, J., Ioannidis, J. P., de Andrade, M., and Rocca, W. A. (2004) UCHL1 is a Parkinson's disease susceptibility gene, *Ann. Neurol. 55*, 512−521.
8. Lowe, J., McDermott, H., Landon, M., Mayer, R. J., and Wilkinson, K. D. (1990) Ubiquitin carboxyl-terminal hydrolase (PGP9.5) is selectively present in ubiquitinated inclusion bodies characteristic of human neurodegenerative diseases, *J. Pathol. 161*, 153−160.
9. Hibi, K., Westra, W. H., Borges, M., Goodman, S., Sidransky, D., and Jen, J. (1999) PGP9.5 as a candidate tumor marker for non-small-cell lung cancer, *Am. J. Pathol. 155*, 711−715.
10. Yamazaki, T., Hibi, K., Takase, T., Tezel, E., Nakayama, H., Kasai, Y., Ito, K., Akiyama, S., Nagasaka, T., and Nakao, A. (2002) PGP9.5 as a marker for invasive colorectal cancer, *Clin. Cancer Res. 8*, 192−195.
11. Tezel, E., Hibi, K., Nagasaka, T., and Nakao, A. (2000) PGP9.5 as a prognostic factor in pancreatic cancer, *Clin. Cancer Res. 6*, 4764−4767.
12. Liu, Y., Lashuel, H. A., Choi, S., Xing, X., Case, A., Ni, J., Yeh, L.-A., Cuny, G. D., Stein, R. L., and Lansbury, P. T., Jr. (2003) Discovery of inhibitors that elucidate the role of UCH-L1 activity in the H1299 lung cancer cell line, *Chem. Biol. 10*, 837−846.
13. Case, A., and Stein, R. L. (2006) Mechanistic studies of ubiquitin C-terminal hydrolase L1, *Biochemistry 45*, 2443−2452.
14. Larsen, C. N., Krantz, B. A., and Wilkinson, K. D. (1998) Substrate specificity of deubiquitinating enzymes: ubiquitin C-terminal hydrolases, *Biochemistry 37*, 3358−3368.
15. Dang, L. C., Melandri, F. D., and Stein, R. L. (1998) Kinetic and mechanistic studies on the hydrolysis of ubiquitin C-terminal 7-amido-4-methylcoumarin by deubiquitinating enzymes, *Biochemistry 37*, 1868−1879.
16. Wilkinson, K. D., Laleli-Sahin, E., Urbauer, J., Larsen, C. N., Shih, G. H., Haas, A. L., Walsh, S. T., and Wand, A. J. (1999) The binding site for UCH-L3 on ubiquitin: mutagenesis and NMR studies on the complex between ubiquitin and UCH-L3, *J. Mol. Biol. 291*, 1067−1077.
17. Misaghi, S., Galardy, P. J., Meester, W. J., Ovaa, H., Ploegh, H. L., and Gaudet, R. (2005) Structure of the ubiquitin hydrolase UCH-L3 complexed with a suicide substrate, *J. Biol. Chem. 280*, 1512−1520.
18. Johnston, S. C., Larsen, C. N., Cook, W. J., Wilkinson, K. D., and Hill, C. P. (1997) Crystal structure of a deubiquitinating enzyme (human UCH-L3) at 1.8 Å resolution, *EMBO J. 16*, 3787−3796.

19. Johnston, S. C., Riddle, S. M., Cohen, R. E., and Hill, C. P. (1999) Structural basis for the specificity of ubiquitin C-terminal hydrolases, *EMBO J. 18*, 3877−3887.
20. Das, C., Hoang, Q. Q., Kreinbring, C. A., Luchansky, S. J., Meray, R. K., Ray, S. S., Lansbury, P. T., Ringe, D., and Petsko, G. A. (2006) Structural basis for conformational plasticity of the Parkinson's disease-associated ubiquitin hydrolase UCH-L1, *Proc. Natl. Acad. Sci. U.S.A. 103*, 4675−4680.
21. Sloper-Mould, K. E., Jemc, J. C., Pickart, C. M., and Hicke, L. (2001) Distinct functional surface regions on ubiquitin, *J. Biol. Chem. 276*, 30483−30489.
22. Larsen, C. N., Price, J. S., and Wilkinson, K. D. (1996) Substrate binding and catalysis by ubiquitin C-terminal hydrolases: identification of two active site residues, *Biochemistry 35*, 6735−6744.
23. Wang, M., Cheng, D., Peng, J., and Pickart, C. M. (2006) Molecular determinants of polyubiquitin linkage selection by an HECT ubiquitin ligase, *EMBO J. 25*, 1710−1719.
24. Morrison, K. L., and Weiss, G. A. (2001) Combinatorial alanine-scanning, *Curr. Opin. Chem. Biol. 5*, 302−307.

BI061406C